



Published in final edited form as:

J Trauma Acute Care Surg. 2022 August 01; 93(2): S110–S118. doi:10.1097/TA.0000000000003674.

A Combat Casualty Relevant Dismounted Complex Blast Injury Model In Swine

Alexis L. Cralley, MD¹, Ernest E. Moore, MD^{1,2}, Daniel Kissau, MD¹, Julia R. Coleman, MD, MPH¹, Navin Vigneshwar, MD¹, Margot DeBot, MD¹, Terry R. Schaid Jr., MD¹, Hunter B. Moore, MD, PhD¹, Mitchell J Cohen, MD¹, Kirk Hansen, PhD¹, Christopher C. Silliman, MD, PhD^{1,5,6}, Angela Sauaia, MD, PhD^{1,3}, Charles J. Fox, MD⁴

¹Department of Surgery, School of Medicine, University of Colorado Denver, Aurora, CO

²Ernest E Moore Shock Trauma Center at Denver Health, Department of Surgery, Denver, CO

³Department of Health Systems, Management and Policy, School of Public Health, University of Colorado Denver

⁴Department of Vascular Surgery, University of Maryland School of Medicine, Baltimore, MD, United States

⁵Vitalant Research Institute, Denver, CO

⁶Department of Pediatrics, School of Medicine, University of Colorado Denver, Aurora, CO

Abstract

Introduction: Improvised explosive devices (IEDs) have resulted in a unique polytrauma injury pattern termed Dismounted Complex Blast Injury (DCBI), which is frequent in the modern military theater. DCBI is characterized by extremity amputations, junctional vascular injury, and blast traumatic brain injury (bTBI). We developed a combat casualty relevant DCBI swine model, which combines hemorrhagic shock (HS) and tissue injury (TI) with a bTBI, to study interventions in this unique and devastating military injury pattern.

Methods: 50kg male Yorkshire swine were randomized to the DCBI or SHAM group (instrumentation only). Those in the DCBI group were subjected to HS, TI, and bTBI. The blast injury was applied using a 55psi shock tube wave. TI was created with bilateral open femur fractures. HS was induced by bleeding from femoral arteries to target pressure. A resuscitation protocol modified from the Tactical Combat Casualty Care guidelines simulated battlefield resuscitation for 240 minutes.

Results: Eight swine underwent the DCBI model and five were allocated to the SHAM group. In the DCBI model the mean base excess (BE) achieved at the end of the HS shock was -8.57 ± 5.13 mmol/L. A significant coagulopathy was detected in the DCBI model as measured

Alexis Cralley: alexis.cralley@dhha.org.

Author Contribution Statement:

A.C., E.M., J.C., M.C., K.H., C.S., A.S., and C.F., conceived and planned the experiments. A.C., E.M., D.K., M.D., T.S., and C.F. carried out the experiments. A.C. performed data collection. A.C and A.S. performed data analysis. A.C., E.M., J.C., M.C., K.H., C.S., and A.S., contributed to the interpretation of the results. A.C. prepared the initial draft of the manuscript and critical revisions were completed by E.M. and A.S. All authors provided critical feedback and helped shape the research, analysis, and manuscript.

by Prothrombin time (PT) (15.8 sec DCBI vs 12.86 sec SHAM, $p=0.02$) and thromboelastography (TEG) maximum amplitude (MA) (68.5mm DCBI vs 78.3mm in SHAM, $p=0.0003$). For the DCBI models ICP increased by a mean 13mmHg reaching a final ICP of 24 ± 7.7 mmHg.

Conclusions: We created a reproducible large animal model to study the combined effects of severe HS, TI, and bTBI on coagulation and intracranial pressure in the setting of DCBI, with significant translational applications for the care of military warfighters. Within the 4-hour observational period swine developed a consistent coagulopathy with a concurrent brain injury evidenced by increasing ICP.

Keywords

Dismounted Complex Blast Injury; Tactical Combat Casualty Care; Polytrauma; Blast Traumatic Brain Injury; Coagulopathy

Introduction

In recent warfare explosions were the most common mechanism of injury, accounting for 78% of casualties and 63% of deaths¹. The resulting complex injury pattern termed dismounted complex blast injury (DCBI) is characterized by an amputation of at least one lower extremity and junctional/urogenital injury leading to hemorrhagic shock (HS), compounded by moderate to severe traumatic brain injury (TBI)². The non-compressible junctional hemorrhagic injuries associated with DCBI result in rapid and extensive blood loss. Uncontrolled hemorrhage resulting from DCBI is the leading cause of death^{1,2} and remains challenging to treat in the austere combat environment³⁻⁵. The life-threatening HS with severe tissue injury following DCBI results in trauma-induced coagulopathy (TIC)^{6,7} characterized by hypocoagulability which further compromises hemostasis⁸.

In addition to the clinically visible injuries due to tissue disruption compounded by TIC, blast forces create overpressures that cause insidious injuries to the viscera, systemic vasculature, and central nervous system (CNS). Blast traumatic brain injuries (bTBI) were previously underappreciated, but have subsequently been associated with cerebral edema, intracranial hemorrhage, and prolonged vasospasms^{9,10}. Furthermore, the interplay of TBI on hemostasis and coagulation is incompletely understood. Clinical studies have shown that TBI can provoke coagulopathy^{11,12}, and coagulopathy combined with TBI results in worse outcomes¹³. However, the interaction of blast injuries and coagulopathy is even less understood as there are few models to evaluate blast on the effects of hemostasis^{14,15}. To optimally treat DCBI, effective resuscitation protocols should prioritize cardiac and cerebral perfusion, reduce blood loss, and restore coagulation homeostasis and mitigate secondary brain injury. Thus, we developed a large animal DCBI model for evaluating resuscitation interventions, such as resuscitative endovascular balloon occlusion of the aorta (REBOA) and tranexamic acid (TXA), which have been proposed as pre-hospital interventions¹⁶ to treat hemorrhagic shock, cardiac and cerebral ischemia, and coagulation following improvised explosive device (IED) related trauma.

Methods

The Institutional Animal Care and Use Committee approved this animal study under protocol #1050. The facility where the research occurred is fully accredited with the Association for Assessment and Accreditation of Laboratory Animal Care International (AAALAC). Research was conducted in compliance with the Animal Welfare Act, implementing Animal Welfare Regulations, the principles of the Guide for the Care and Use of Laboratory Animals, National Research Council, and reported in accordance with the ARRIVE guidelines. The checklist of the ARRIVE guidelines used to ensure proper reporting of the methods, results, and discussion are included in the supplemental digital content (SDC 1). Thirteen healthy adolescent male Yorkshire swine (45-56 kg) were acclimated for a minimum of 3 days prior to experimental procedures.

Anesthesia:

Anesthesia is induced initially via intramuscular injection with ketamine (20.0 mg/kg), xylazine (2.0 mg/kg), and acepromazine (0.2 mg/kg) followed by intubation under direct laryngoscopy. Continuous infusion anesthesia using propofol (3 mg/kg/hr) and fentanyl (3 mcg/kg/hr) is maintained throughout the experiment using a superficial ear vein. SHAM animals are sedated under the same anesthesia protocol and undergo the same vascular access but do not undergo any injuries. The DCBI model is summarized in Figure 1.

Monitoring:

An intracranial pressure (ICP) monitor (Integra LifeSciences, Plainsboro, NJ) is placed in the subdural space of the left frontal lobe (SDC 2). A 10mm burr hole is drilled 1cm from midline and 1cm above the brow line for insertion into the left frontal lobe. Arterial vascular access is established for invasive blood pressure monitoring.

Axillary Artery Vascular Access:

Instrumentation begins with obtaining an arterial line for blood sampling and invasive blood pressure monitoring. The right forelimb of the supine swine is placed in full extension at 90 degrees. After identifying the brachial pulse via digital palpation, an 8cm longitudinal incision is made. Blunt dissection of the loose areolar tissue allows for visualization and isolation of the artery, vein, and median nerve. A 5 Fr micropuncture sheath is utilized and connected to the arterial pressure line (SDC 3).

Blast Injury:

The bTBI is created with a Friedlander type blast wave using a compressed gas mobile shock tube (MST). The mobile shock tube is housed in an outdoor 52-foot trailer and managed by Applied Research Associates, Inc. (Littleton, CO) and swine are transported from the Vivarium operating room to the MST for the blast injury. A National Institute of Justice (NIJ) Level II vest, ear plugs, and goggles are placed on the swine in the operative room to limit unwanted blast exposure to the torso, eyes, and ears (SDC 4). Targeted peak pressure for the TBI is 55psi with an associated positive phase duration spanning 3 to 5 milliseconds.

Femoral Arterial and Venous Access:

Due to the manipulation and force of the blast injury, no further vascular access is obtained until after the bTBI. Prior to the tissue injury, both femoral arteries are cannulated percutaneously and one femoral vein is cannulated. Using ultrasound (US) guidance with the Seldinger technique¹⁷, we place 0.018” stainless steel wires into both femoral arteries and one femoral vein. Placement of all wires prior to the cannulas improves the clarity of the US image and allows for easier needle access to each vessel without interference of any large sheaths already placed. In the femoral vein a large sheath (10 Fr) suitable for rapid blood product resuscitation is placed. A 7 Fr introducer sheath is inserted into one femoral artery. A 12 Fr pediatric extracorporeal membrane oxygenation (ECMO) cannula is placed in the other femoral artery for rapid, controlled bleeding during the hemorrhagic shock phase (SDC 5).

Tissue Injury:

Surgical cutdown through the skin and quadriceps of the extended hind limbs is done until the femur is visualized. A captive bolt stunner (Blitz-Kerner, Turbocut JOBB GmbH, Germany) is placed directly on each femur and confirmed with visualization. Following the firing of the stun gun against the femur, visual inspection and digital palpation is used to confirm femur fracture (SDC 5). Fractured femurs are packed with gauze to minimize blood loss from fracture site.

Hemorrhagic Shock:

Fixed-pressure hemorrhagic shock is initiated by bleeding from the 12Fr femoral arterial catheter. Shed blood is removed into citrated 450mL blood transfusion bags (Jorgensen Laboratories, Inc. Loveland, CO). The target mean arterial pressure (MAP) within 10 minutes is 20mmHg. Once 20 mmHg is obtained, blood removal is titrated to maintain a MAP of 15 mmHg and an end-tidal carbon dioxide (EtCO₂) of 20 mmHg. When swine reach the MAP and EtCO₂ goals, they are maintained at these levels by titrating further blood loss to maintain these endpoints. Amiodarone (150mg) is administered to prevent ventricular arrhythmias. Base excess readings every 5-10 minutes are further used to titrate blood removal and confirm adequate depth of shock. Swine are maintained at this pressure range for 30-45 minutes until the base excess (BE) reaches -10 mmol/L. The amount of blood volume percentage removed during shock is calculated using the standard volume of 66mL/kg¹⁸.

Resuscitation:

At the end of HS, resuscitation is initiated following a modified combat casualty care protocol. The resuscitation and post injury monitoring period is continued for 240 minutes. The target MAP for the 1st hour of resuscitation is 35 mmHg, representing limited fluid transfusion capacity in an austere combat environment. Once the pig reaches the 2nd hour of resuscitation the MAP goal is maintained >60 mmHg. Resuscitation begins with 500mL of 5% human albumin (Grifols Biologicals Inc., Los Angeles, CA), followed by one unit of shed blood. A bolus of 1 gm 10% calcium chloride is given with the first unit of blood transfused. After the 1st unit of shed blood another 500mL of 5% human albumin

is used. The remainder of the resuscitation period includes the shed blood bags, with calcium administered with each subsequent unit of shed blood. Pigs are euthanized using pentobarbital (86.6mg/kg) at the conclusion of the experiment at 240min post injury.

Data Collection and Analysis:

Vital signs including blood pressure, MAP, heart rate (HR), respiratory rate (RR), and EtCO₂ are monitored continuously and recorded every 5 minutes. ICP is monitored continuously and recorded every 5 minutes. At prespecified timepoints (Figure 1), arterial blood is collected for citrate native (CN) and tissue plasminogen activator (tPA)-challenge thrombelastography (TEG), complete blood cell count (CBC), lipase, creatinine, total bilirubin, and troponin to assess organ dysfunction. A previously described tPA-challenge TEG has been developed to overcome the swine's innate resistant to tPA-catalyzed lysis¹⁹. Prior work has shown that a final concentration of 1500ng/mL of swine tPA added to the TEG cup provides enough exogenous tPA to overcome this resistance to elicit lysis on TEG. CN TEG results include the speed of clot initiation (R-time), rate of clot propagation (angle), maximum clot strength (maximum amplitude, MA), and percent lysis at 30 minutes (LY30). Only LY30 is analyzed in the tPA-challenge TEG. Whole blood is used for point of care analysis of blood gases and PT/INR with an iSTAT-1 point of care analyzer and CG8+ and PT/INR Cartridges (Abbott Point of Care Inc., Princeton, NJ). Brain water content is calculated using a validated wet-to-dry protocol after brains are weighed, then dried at 100°C for 48 hours and reweighed^{20,21}.

Data were inputted into Microsoft Excel 2010 (Microsoft Corporation, Redmond, USA) and analyzed using SAS Studio 2021 and SAS vs 9.4 (SAS Institute, Cary, NC). Linear mixed models for repeated measures are used to compare the temporal trends of the groups, with contrasts between groups adjusted by using the false discovery rate method. Sample size and power was calculated prior to performing all animal models using expected CN TEG MA, CN TEG LY30, and ICP outcomes. With 80% power and 95% confidence to detect a minimum change of 4.0mm in MA and a minimum difference of 3 percentage points in LY30, a minimum of 5 animals per group were required. With a baseline mean ICP of 11.5mmHg and standard deviation of 2.9²², a sample size of 5 pigs with significance level of 0.05 allows for detection of a minimum change in ICP of 5.9 mm Hg. A p-value than 0.05 was considered statistically significant. Correlations were conducted with the Pearson correlation test. Distribution analysis was by visually inspecting histograms. For variables not normally distributed, a Box-Cox power transformation was performed prior to analysis. Data are presented as mean \pm standard deviation or median \pm interquartile range unless otherwise noted.

Results

Eight swine were allocated to the DCBI model and five swine to the SHAM model. No SHAM swine expired during the experiment, while one of the 8 DCBI swine expired early (12% mortality) during the early HS phase. Baseline physiology was similar between the groups (SDC 6).

Model goals:

For the bTBI, the mean blast over pressure for all DCBI pigs was 53.0 ± 1.8 psi. For the HS phase, the mean time that swine remained in shock to achieve the target BE was 56.1 ± 27.9 minutes. Two out of the eight DCBI swine (25%) required immediate resuscitation prior to the BE goal due to agonal breathing and rapidly declining MAP and EtCO₂. The resuscitation of these swine followed the same protocol as all others. One of these swine expired immediately despite resuscitation. The other swine survived to completion and its time spent in the HS phase and final BE were similar to the other DCBI models ($p > 0.2$). The mean BE achieved at the end of the HS in the DCBI models was -8.6 ± 5.1 mmol/L compared to a BE of 10.8 ± 2.6 for the SHAM models at the same time. This represented a mean change from baseline BE of 18.2 mmol/L for the DCBI group. The BE achieved correlated with the amount of shed blood ($r = -0.84$, $p = 0.0006$). To achieve this level of HS, the mean blood volume removed from the 8 DCBI swine was $46 \pm 11\%$ of the total blood volume. During HS, the DCBI model had significant decreases in their MAP within the first 15 minutes of controlled bleeding (MAP 15.5 ± 3.3 mmHg vs 64.6 ± 14.4 , $p = 0.0003$). Critically low MAP and EtCO₂ were maintained throughout shock.

Resuscitation:

At the conclusion of HS phase, resuscitation with albumin and shed blood slowly increased the blood pressures and EtCO₂ progressively. At the completion of the model at 240min post injury, MAP, EtCO₂, and HR returned to their baseline levels and were similar to that of the SHAM models (Figure 2).

Cardiac and Visceral Organ Function:

The DCBI produced no significant changes in electrolyte levels compared to SHAM models. Calcium levels decreased slightly during shock despite calcium replacement. Glucose levels for SHAM models remained unchanged, but decreased after resuscitation in DCBI swine until the 240min endpoint ($p < 0.01$) and at the end of the model was significantly lower compared to SHAM (82.3 ± 15.1 mg/dL vs 126 ± 15.3 , $p = 0.01$) (SDC 7). Troponin, total bilirubin, and creatinine increased significantly from baseline in the DCBI model but did not change in the SHAM models ($p < 0.05$). The final levels of troponin, total bilirubin, and creatinine were elevated significantly in the DCBI models compared to SHAM ($p < 0.05$). Lipase remained constant in both models ($p < 0.05$), but at final lipase was lower in the DCBI group than SHAM (Figure 3).

Cerebral Perfusion:

Intracranial pressure and cerebral perfusion pressure are shown in Figure 4. Baseline ICPs were similar in the two models, but after the completion of the HS phase and beginning of resuscitation, the ICPs of DCBI animals increased steadily and significantly until the end of the model at 240min, when the final ICP was 24 ± 7.7 mmHg compared to SHAM model ICP of 7 ± 8.4 , $p = 0.0007$. ICPs of the SHAM pigs remained constant throughout the model. Corresponding cerebral perfusion pressure (CPP) in the DCBI models was significantly lower than the SHAM models during shock and until 180min post injury. Brain weight edema assessments showed a trend of increased water content (gram of water/gram of dry

tissue), representing edema in the DCBI model compared to the SHAM model (3.9 ± 0.4 g vs 3.8 ± 0.0 g water/gram of dry tissue, $p=0.6$).

Coagulopathy:

Coagulopathy measured by CN TEGs was indicated by a persistent decrease in MA (a measurement of clot strength) in the DCBI compared to SHAM (Figure 5). The decrease in MA was significantly correlated with the lowest BE achieved ($r=0.86$, $p=0.0002$) and the amount of blood removed from the swine ($r=-0.75$, $p=0.005$). There were no significant changes from baseline in the CN TEG R-time, angle, and LY30 in both groups. For the tPA-challenge TEG, the DCBI model produced significant fibrinolysis at 30 and 60min post HS (Figure 6).

A significant coagulopathy was detected in the DCBI model as measured by PT (Figure 6). PT increased throughout the HS shock phase and peaked at 30min post injury and into resuscitation (15.8 ± 2.4 sec DCBI vs 12.9 ± 0.6 sec SHAM, $p=0.02$). There were no significant changes in PT throughout the SHAM model. The maximum PT reached was significantly correlated with the lowest BE ($r=-0.78$, $p=0.003$) achieved, and the amount of blood loss required to achieve that level of HS ($r=0.65$, $p=0.02$). At 240min post injury, the mean PT for the DCBI model returned to near baseline value and was not significantly different from the SHAM PT. Compared to SHAM, DCBI swine produced a steadily declining platelet count from a baseline of $378 \times 10^9/L$ until the end of model at 240min, reaching $208 \times 10^9/L$ ($p=0.0003$).

Discussion

Animal models are essential to evaluate HS-induced TIC and TBI resuscitation strategies, but few models have employed polytrauma (tissue injury and hypoperfusion), and fewer incorporate TBI. Previously described military relevant polytrauma models include a noncompressible torso hemorrhage model²³, a multicenter lethal triad model (consisting of acidosis, hypothermia, and dilutional coagulopathy)²⁴, and an intra-abdominal sepsis model incorporating TBI²⁵. Our newly created model focuses on DCBI with TBI, TI, and HS; thus incorporating additional challenges that TBI contributes to shock resuscitation and vice versa. Secondary insults such as hypotension, hypoxia, and inflammation lead to additional neurological injury and worsen secondary brain injury^{26,27}. Hypotension increases mortality by 150% in severe TBI cases²⁸. Additionally, coagulopathy combined with TBI, which is present in one-third of these patients, is associated with worse outcomes^{29,30}. Clinical findings indicate TBI combined with HS is associated with prolonged PT and decreased platelet counts¹². Clinical reports and swine models incorporating isolated HS or TBI compared to combined HS+TBI and controlled cortical impact models suggest that hypotension must be present for coagulopathy to develop following TBI^{26,31}. Our polytrauma model showed similar results, indicating a hypocoagulable state following DCBI with prolonged PT, reduced MA, and thrombocytopenia. *Cho et al* also showed increasing PT and declining MA in their multicenter polytrauma swine model; however, their use of normal saline (NS) creates a dilutional coagulopathy²⁴. Other previous military-relevant polytrauma models utilized NS^{23,25}, however we avoided NS to prevent dilutional

coagulopathy and instead evaluate iatrogenic TIC. Thus the increasing PT and decreasing MA levels are significantly correlated with greater blood loss and deeper shock leading to TIC. This finding that the degree of coagulopathy is influenced by the level of hemorrhagic shock is consistent with other large animal models^{26,31}. However, in rodent models isolated HS is not associated with changes in MA³². We previously evaluated TEG changes in 572 trauma patients with and without TBI and found that severe TBI had no association with changes in MA; however, lower MA was observed in patients with TBI and TI compared to isolated TBI and isolated TI¹¹. The significant decrease in MA seen in this DCBI model is likely due to the interactions of the bTBI with HS and severe TI, resulting from not only decreased platelet count but also platelet dysfunction secondary to TBI³³.

Measuring hyperfibrinolysis in swine models is difficult as swine are hypercoagulable and resistant to tPA-driven lysis³⁴. The tPA challenge assay is designed to unmask latent hyperfibrinolysis.³⁵ The tPA challenge TEG utilizes 1500 ng/ml of swine tPA *ex-vivo* to achieve a detectable level of lysis on TEG. While increases in LY30 on the tPA challenge TEG did not reach significance given the small sample sizes, the data suggest that DCBI promotes a hyperfibrinolytic state. In clinical studies, tissue hypoperfusion and ischemia are associated with early coagulopathy associated with hyperfibrinolysis³⁶⁻³⁸. Rodent work indicates shock stimulates fibrinolysis, while tissue injury provokes fibrinolytic shutdown³⁹. Recent clinical studies suggest TBI promotes fibrinolysis shutdown⁴⁰. Consequently, DCBI's unique injury profile with severe TBI, TI, and life-threatening HS is important to discern the overall balance in fibrinolysis regulation. In our DCBI model incorporating severe blood loss of nearly 50% of total blood volume indicated a tendency to increase lysis.

The severe level of shock we were able to produce in this model is evident by visceral organ damage detected by increases in creatinine and total bilirubin levels. While the changes detected may not be considered clinically important in this acute four-hour model, even these small changes increase the risk of developing multiple organ failure following DCBI, especially if a patient's fibrinolytic phenotype favors shutdown over hyperfibrinolysis⁴¹.

This unique DCBI animal model is also unlike previous polytrauma animal models which employ cortical impact devices to produce a TBI. Instead, our model employs a whole-body blast insult to produce the blast specific TBI. Blast insults are the leading cause of TBI in the combat theater, accounting for 64% of all TBIs in Iraq and 47% of TBIs incurred in Afghanistan⁴². The widespread use of Kevlar vests mitigates the torso insult from blast and protect the head and chest from penetrating trauma^{43,44}. However, even with body armor uncontrolled hemorrhage often results in death before reaching a treatment facility, and the effects of prolonged hypotension on the blast brain injury are not well characterized^{2,3,45}. In order to study the primary blast injury and its effect on the brain and TIC we utilized a combat relevant whole-body blast exposure produced by a specially developed blast tube which generates a Friedlander-type blast wave similar to that produced by explosions in combat theater⁴⁶. To further reproduce a military scenario and limit life-threatening barotrauma to the lungs, swine wear a military grade Kevlar vest which serves to minimize damage to the lungs and gastrointestinal tract, as these air-containing organs are most susceptible to damage following dramatic high-pressure changes⁴⁷.

To our knowledge this is the only bTBI model capturing ICPs and CPPs throughout the model. After the bTBI and during HS, ICPs remained relatively stable. It was not until 1 hour into resuscitation that ICPs began to increase steadily, reaching statistically significant higher values than baseline. The mean increase from baseline for the DCBI model was 12.4mmHg, representing a doubling from the baseline value of 11.1mmHg. The delayed rise in ICPs may be due to the loss of autoregulation following the bTBI and brain ischemia. The CPPs recorded during the HS phase were consistently <5mmHg after the first 15min of shock, representing dangerously low brain perfusion. The Brain Trauma Foundation recommends a CPP range of 60-70 mmHg as optimal targets for treating TBI, and ICP elevations above 22mmHg are considered the threshold associated with poor outcomes⁴⁸. In this swine DCBI model, an acceptable CPP was not achieved until 120min after shock and resuscitation. At 120min, CPP for the DCBI group reached a mean 43.2mmHg, and the ICP was below the 22mmHg threshold, at 17.8mmHg. However, continued resuscitation to reach a MAP >60mmHg and a SBP >100mmHg resulted in further ICP increases above the 22mmHg threshold. Thus, this model highlights the complex resuscitation strategies needed to treat life threatening hemorrhage and bTBI. Our results, combined with Garner's data in which there was a 0% survival rate in a swine model with controlled hemorrhage and primary blast injury when treated with permissive hypotension, suggest there is a delicate balance between optimal resuscitation and progressive secondary brain injury⁴⁹.

The standardization and reproducibility of this model to detect visceral ischemia, coagulopathy, and cerebral perfusion changes following DCBI and throughout resuscitation is important in establishing a baseline injury threshold. Moving forward, this model serves as the foundation to introduce additional interventions and evaluate their effects on these same parameters. Interventions such as REBOA to control bleeding, TXA to correct hyperfibrinolysis, and hypertonic saline to decrease ICP could be introduced in future iterations. Additionally novel devices or drugs still in the preclinical phase with potential use in Tactical Combat Casualty Care scenarios or blast injuries could be vetted through a well-established model like this.

Limitations of this animal model include the short monitoring time for observation due to our local animal care facility restrictions. The 4-hour model allows us to study the immediate effects following DCBI but we are unable to extrapolate findings beyond the acute injury period. Unfortunately, prolonged models evaluating outcomes at 24 and 48 hours are cost-prohibitive when balancing adequate sample sizes providing efficient power, especially when considering the need to account for early mortality in a highly lethal model. The model was powered to detect changes in coagulopathy and ICP. While we detected significant changes in MA and ICP, we were not able to detect significant changes in CN LY30 values. However, the tPA challenge TEG targeted to overcome swine blood resistance to tPA-catalyzed lysis was able to detect challenges. Additionally, this model replicates a modern combat theater injury in which HS, severe tissue injury, and bTBI frequently occur together after encounter with an IED. The clinical relevance of this model should be interpreted within that injury scope. Differences within species are also relevant when interpreting the results, especially in the setting of TBI animal models in which brain anatomy and skull thickness effect our ability to replicate human TBI. However, limitations are inherent to all animal models, and our findings provide new insight into the

coagulopathy and brain injury following such a complex military injury. Lastly, recreation of a complex blast trauma models must consider the logistical challengers of safety deploying blast waves in research settings. Significant administrative oversight, logistical timelines, and safety protocols all need to be incorporated into the scientific model to achieve success.

In conclusion, we have created a reproducible, large animal model composed of bTBI, severe TI, and HS. This model adds to the previously published military relevant, swine polytrauma models by incorporating DCBI with noncompressible hemorrhage below the torso. Our model produces a consistent coagulopathy, measurable by PT and MA by TEG. The model provides evidence of evolving brain injury through continuous intracranial pressure monitoring. This model will serve as the baseline cohort to introduce additional resuscitation strategies to treat DCBI.

Supplementary Material

Refer to Web version on PubMed Central for supplementary material.

Support:

This research is funded by the Department of Defense contract number W81XWH2010205.

References

1. Cannon JW, Hofmann LJ, Glasgow SC, Potter BK, Rodriguez CJ, Cancio LC, et al. Dismounted Complex Blast Injuries: A Comprehensive Review of the Modern Combat Experience. *J Am Coll Surg.* Oct 2016;223(4):652–664 e658. [PubMed: 27481095]
2. Eastridge BJ, Mabry RL, Seguin P, Cantrell J, Tops T, Uribe P, et al. Death on the battlefield (2001-2011): implications for the future of combat casualty care. *J Trauma Acute Care Surg.* Dec 2012;73(6 Suppl 5):S431–437. [PubMed: 23192066]
3. Morrison JJ, Stannard A, Rasmussen TE, Jansen JO, Tai NR, Midwinter MJ. Injury pattern and mortality of noncompressible torso hemorrhage in UK combat casualties. *J Trauma Acute Care Surg.* Aug 2013;75(2 Suppl 2):S263–268. [PubMed: 23883918]
4. Northern DM, Manley JD, Lyon R, Farber D, Mitchell BJ, Filak KJ, et al. Recent advances in austere combat surgery: Use of aortic balloon occlusion as well as blood challenges by special operations medical forces in recent combat operations. *J Trauma Acute Care Surg.* Jul 2018;85(1S Suppl 2):S98–S103. [PubMed: 29787545]
5. Rees P. Response to: 'REBOA at Role 2 Afloat: resuscitative endovascular balloon occlusion of the aorta as a bridge to damage control surgery in the military maritime setting' by Rees et al. *J R Army Med Corps.* Jun 2019;165(3):213–214. [PubMed: 30127069]
6. Brohi K, Singh J, Heron M, Coats T. Acute traumatic coagulopathy. *J Trauma.* Jun 2003;54(6):1127–1130. [PubMed: 12813333]
7. Kashuk JL, Moore EE, Sawyer M, Wohlauser M, Pezold M, Barnett C, et al. Primary fibrinolysis is integral in the pathogenesis of the acute coagulopathy of trauma. *Ann Surg.* Sep 2010;252(3):434–442; discussion 443–434. [PubMed: 20739843]
8. Moore EE, Moore HB, Kornblith LZ, Neal MD, Hoffman M, Mutch NJ, et al. Trauma-induced coagulopathy. *Nat Rev Dis Primers.* Apr 29 2021;7(1):30. [PubMed: 33927200]
9. Armonda RA, Bell RS, Vo AH, Ling G, DeGraba TJ, Crandall B, et al. Wartime traumatic cerebral vasospasm: recent review of combat casualties. *Neurosurgery.* Dec 2006;59(6):1215–1225; discussion 1225. [PubMed: 17277684]
10. Ling G, Bandak F, Armonda R, Grant G, Ecklund J. Explosive blast neurotrauma. *J Neurotrauma.* Jun 2009;26(6):815–825. [PubMed: 19397423]

11. Samuels JM, Moore EE, Silliman CC, Banerjee A, Cohen MJ, Ghasabyan A, et al. Severe traumatic brain injury is associated with a unique coagulopathy phenotype. *J Trauma Acute Care Surg.* Apr 2019;86(4):686–693. [PubMed: 30601456]
12. Galvagno SM Jr., Fox EE, Appana SN, Baraniuk S, Bosarge PL, Bulger EM, et al. Outcomes after concomitant traumatic brain injury and hemorrhagic shock: A secondary analysis from the Pragmatic, Randomized Optimal Platelets and Plasma Ratios trial. *J Trauma Acute Care Surg.* Oct 2017;83(4):668–674. [PubMed: 28930959]
13. de Oliveira Manoel AL, Neto AC, Veigas PV, Rizoli S. Traumatic brain injury associated coagulopathy. *Neurocrit Care.* Feb 2015;22(1):34–44. [PubMed: 25052157]
14. Prima V, Serebruany VL, Svetlov A, Hayes RL, Svetlov SI. Impact of moderate blast exposures on thrombin biomarkers assessed by calibrated automated thrombography in rats. *J Neurotrauma.* Nov 15 2013;30(22):1881–1887. [PubMed: 23805797]
15. Prat NJ, Montgomery R, Cap AP, Dubick MA, Sarron JC, Destombe C, et al. Comprehensive evaluation of coagulation in swine subjected to isolated primary blast injury. *Shock.* Jun 2015;43(6):598–603. [PubMed: 25643012]
16. TCCC Guidelines for Medical Personnel- 1 August 2019. website. https://jts.amedd.army.mil/assets/docs/cpgs/Prehospital_En_Route_CPGs/Tactical_Combat_Casualty_Care_Guidelines_01_Aug_2019.pdf. Updated Accessed 7 May 2020.
17. Seldinger SI. Catheter replacement of the needle in percutaneous arteriography; a new technique. *Acta radiol.* May 1953;39(5):368–376. [PubMed: 13057644]
18. Russo RM, Neff LP, Lamb CM, Cannon JW, Galante JM, Clement NF, et al. Partial Resuscitative Endovascular Balloon Occlusion of the Aorta in Swine Model of Hemorrhagic Shock. *J Am Coll Surg.* Aug 2016;223(2):359–368. [PubMed: 27138649]
19. Moore HB, Moore EE, Gonzalez E, Hansen KC, Dzieciatkowska M, Chapman MP, et al. Hemolysis exacerbates hyperfibrinolysis, whereas plateletolysis shuts down fibrinolysis: evolving concepts of the spectrum of fibrinolysis in response to severe injury. *Shock.* Jan 2015;43(1):39–46. [PubMed: 25072794]
20. Elliott MB, Jallo JJ, Tuma RF. An investigation of cerebral edema and injury volume assessments for controlled cortical impact injury. *J Neurosci Methods.* Mar 15 2008;168(2):320–324. [PubMed: 18076998]
21. Keep RF, Hua Y, Xi G. Brain water content. A misunderstood measurement? *Transl Stroke Res.* Jun 2012;3(2):263–265. [PubMed: 22888371]
22. Hawryluk GW, Phan N, Ferguson AR, Morabito D, Derugin N, Stewart CL, et al. Brain tissue oxygen tension and its response to physiological manipulations: influence of distance from injury site in a swine model of traumatic brain injury. *J Neurosurg.* Nov 2016;125(5):1217–1228. [PubMed: 26848909]
23. White JM, Cannon JW, Stannard A, Spencer JR, Hancock H, Williams K, et al. A porcine model for evaluating the management of noncompressible torso hemorrhage. *J Trauma.* Jul 2011;71(1 Suppl):S131–138. [PubMed: 21795889]
24. Cho SD, Holcomb JB, Tieu BH, Englehart MS, Morris MS, Karahan ZA, et al. Reproducibility of an animal model simulating complex combat-related injury in a multiple-institution format. *Shock.* Jan 2009;31(1):87–96. [PubMed: 18497710]
25. O'Connell RL, Wakam GK, Siddiqui A, Williams AM, Graham N, Kemp MT, et al. Development of a large animal model of lethal polytrauma and intra-abdominal sepsis with bacteremia. *Trauma Surg Acute Care Open.* 2021;6(1):e000636. [PubMed: 33537457]
26. Sillesen M, Rasmussen LS, Jin G, Jepsen CH, Imam A, Hwabejire JO, et al. Assessment of coagulopathy, endothelial injury, and inflammation after traumatic brain injury and hemorrhage in a porcine model. *J Trauma Acute Care Surg.* Jan 2014;76(1):12–19; discussion 19–20. [PubMed: 24368352]
27. Lannoo E, Van Rietvelde F, Colardyn F, Lemmerling M, Vandekerckhove T, Jannes C, et al. Early predictors of mortality and morbidity after severe closed head injury. *J Neurotrauma.* May 2000;17(5):403–414. [PubMed: 10833059]

28. Chesnut RM, Marshall LF, Klauber MR, Blunt BA, Baldwin N, Eisenberg HM, et al. The role of secondary brain injury in determining outcome from severe head injury. *J Trauma*. Feb 1993;34(2):216–222. [PubMed: 8459458]
29. Harhangi BS, Kompanje EJ, Leebeek FW, Maas AI. Coagulation disorders after traumatic brain injury. *Acta Neurochir (Wien)*. Feb 2008;150(2):165–175; discussion 175. [PubMed: 18166989]
30. Wafaisade A, Lefering R, Tjardes T, Wutzler S, Simanski C, Paffrath T, et al. Acute coagulopathy in isolated blunt traumatic brain injury. *Neurocrit Care*. Apr 2010;12(2):211–219. [PubMed: 19806475]
31. Cohen MJ, Brohi K, Ganter MT, Manley GT, Mackersie RC, Pittet JF. Early coagulopathy after traumatic brain injury: the role of hypoperfusion and the protein C pathway. *J Trauma*. Dec 2007;63(6):1254–1261; discussion 1261–1252. [PubMed: 18212647]
32. Harr JN, Moore EE, Wohlauser MV, Droz N, Fragoso M, Banerjee A, et al. The acute coagulopathy of trauma is due to impaired initial thrombin generation but not clot formation or clot strength. *J Surg Res*. Oct 2011;170(2):319–324. [PubMed: 21550061]
33. Castellino FJ, Chapman MP, Donahue DL, Thomas S, Moore EE, Wohlauser MV, et al. Traumatic brain injury causes platelet adenosine diphosphate and arachidonic acid receptor inhibition independent of hemorrhagic shock in humans and rats. *J Trauma Acute Care Surg*. May 2014;76(5):1169–1176. [PubMed: 24747445]
34. Stettler GR, Moore EE, Moore HB, Lawson PJ, Fragoso M, Nunns GR, et al. Thrombelastography indicates limitations of animal models of trauma-induced coagulopathy. *J Surg Res*. Sep 2017;217:207–212. [PubMed: 28583756]
35. Moore HB, Moore EE, Gonzalez E, Chapman MP, Chin TL, Silliman CC, et al. Hyperfibrinolysis, physiologic fibrinolysis, and fibrinolysis shutdown: the spectrum of postinjury fibrinolysis and relevance to antifibrinolytic therapy. *J Trauma Acute Care Surg*. Dec 2014;77(6):811–817; discussion 817. [PubMed: 25051384]
36. Brohi K, Cohen MJ, Ganter MT, Matthay MA, Mackersie RC, Pittet JF. Acute traumatic coagulopathy: initiated by hypoperfusion: modulated through the protein C pathway? *Ann Surg*. May 2007;245(5):812–818. [PubMed: 17457176]
37. Moore EE, Moore HB, Gonzalez E, Sauaia A, Banerjee A, Silliman CC. Rationale for the selective administration of tranexamic acid to inhibit fibrinolysis in the severely injured patient. *Transfusion*. Apr 2016;56 Suppl 2:S110–114. [PubMed: 27100746]
38. Schochl H, Cadamuro J, Seidl S, Franz A, Solomon C, Schlimp CJ, et al. Hyperfibrinolysis is common in out-of-hospital cardiac arrest: results from a prospective observational thromboelastometry study. *Resuscitation*. Apr 2013;84(4):454–459. [PubMed: 22922072]
39. Moore HB, Moore EE, Lawson PJ, Gonzalez E, Fragoso M, Morton AP, et al. Fibrinolysis shutdown phenotype masks changes in rodent coagulation in tissue injury versus hemorrhagic shock. *Surgery*. Aug 2015;158(2):386–392. [PubMed: 25979440]
40. Meizoso JP, Moore HB, Moore EE, Gilna GP, Ghasabyan A, Chandler J, et al. Traumatic Brain Injury Provokes Low Fibrinolytic Activity in Severely Injured Patients. *J Trauma Acute Care Surg*. Feb 14 2022.
41. Moore EE, Moore HB, Gonzalez E, Chapman MP, Hansen KC, Sauaia A, et al. Postinjury fibrinolysis shutdown: Rationale for selective tranexamic acid. *J Trauma Acute Care Surg*. Jun 2015;78(6 Suppl 1):S65–69. [PubMed: 26002266]
42. Wang EW, Huang JH. Understanding and treating blast traumatic brain injury in the combat theater. *Neurol Res*. Apr 2013;35(3):285–289. [PubMed: 23336263]
43. Wade AL, Dye JL, Mohrle CR, Galarneau MR. Head, face, and neck injuries during Operation Iraqi Freedom II: results from the US Navy-Marine Corps Combat Trauma Registry. *J Trauma*. Oct 2007;63(4):836–840. [PubMed: 18090014]
44. Xydakis MS, Fravell MD, Nasser KE, Casler JD. Analysis of battlefield head and neck injuries in Iraq and Afghanistan. *Otolaryngol Head Neck Surg*. Oct 2005;133(4):497–504. [PubMed: 16213918]
45. Holcomb J, Caruso J, McMullin N, Wade CE, Pearse L, Oetjen-Gerdes L, et al. Causes of death in US Special Operations Forces in the global war on terrorism: 2001–2004. *US Army Med Dep J*. Jan-Mar 2007:24–37. [PubMed: 20084703]

46. Bauman RA, Ling G, Tong L, Januszkiewicz A, Agoston D, Delanerolle N, et al. An introductory characterization of a combat-casualty-care relevant swine model of closed head injury resulting from exposure to explosive blast. *J Neurotrauma*. Jun 2009;26(6):841–860. [PubMed: 19215189]
47. Rafaels K, Bass CR, Salzar RS, Panzer MB, Woods W, Feldman S, et al. Survival risk assessment for primary blast exposures to the head. *J Neurotrauma*. Nov 2011;28(11):2319–2328. [PubMed: 21463161]
48. Carney N, Totten AM, O'Reilly C, Ullman JS, Hawryluk GW, Bell MJ, et al. Guidelines for the Management of Severe Traumatic Brain Injury, Fourth Edition. *Neurosurgery*. Jan 1 2017;80(1):6–15. [PubMed: 27654000]
49. Garner J, Watts S, Parry C, Bird J, Cooper G, Kirkman E. Prolonged permissive hypotensive resuscitation is associated with poor outcome in primary blast injury with controlled hemorrhage. *Ann Surg*. Jun 2010;251(6):1131–1139. [PubMed: 20485127]

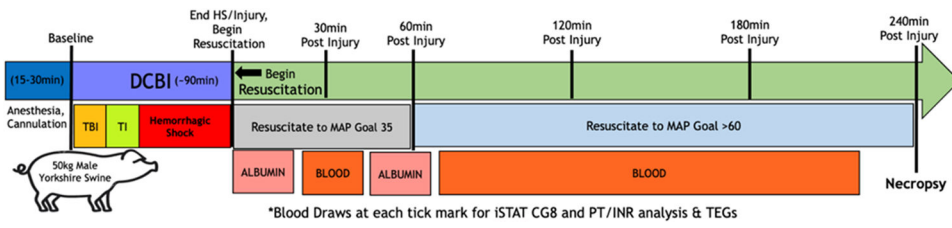


Figure 1. Graphical representation of experiment.

Following anesthesia and initial vascular and intracranial access, swine were either subjected a SHAM model (consisting of surgical access and instrumentation only) or to the dismantled complex blast injury (DCBI: consisting of blast TBI, tissue injury caused by bilateral femur fractures, and then a pressure targeted hemorrhagic shock phase). The SHAM group remained under anesthesia and monitored during the time it takes to complete the entire DCBI series. At the end of the hemorrhagic shock phase, DCBI swine are monitored for 240min during which resuscitation occurs. SHAM swine complete 240min of observation with normal saline for fluid replacement for insensible losses.

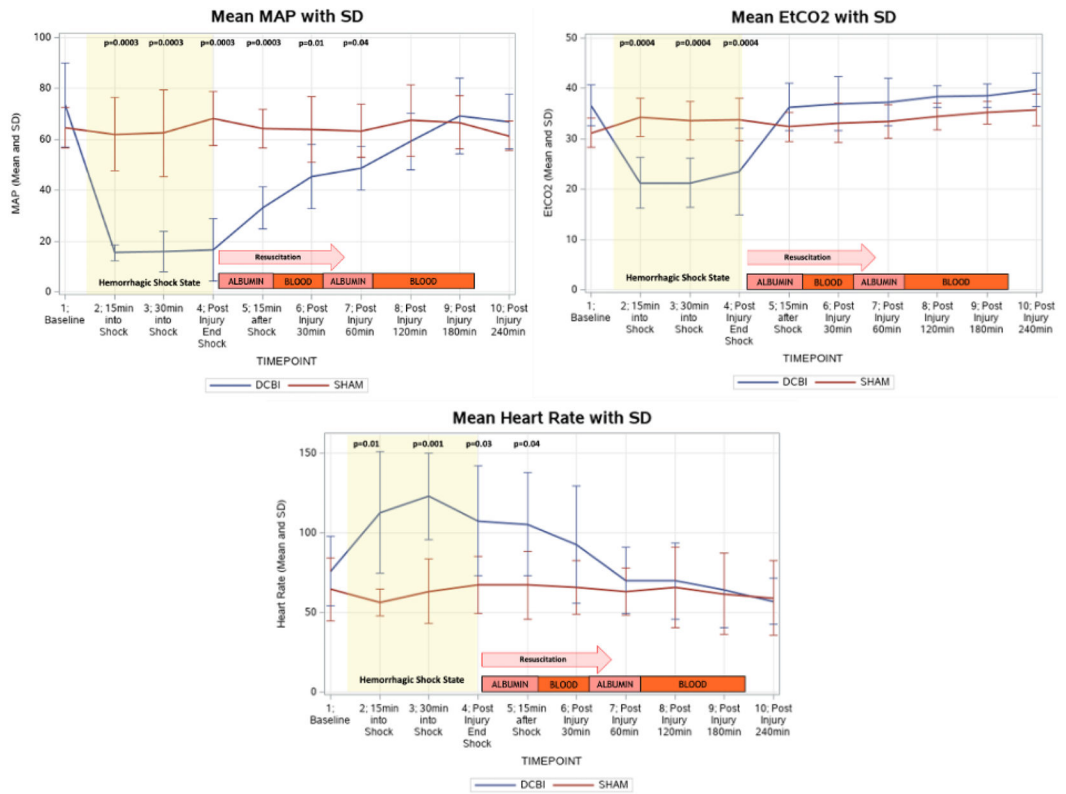


Figure 2. The MAP, EtCO₂, and heart rate changes monitored throughout the model are shown. DCBI swine are subjected to blood removal to until MAP reaches 15-20mmHg and EtCO₂ decreased to 20mmHg. Heart rate subsequently increases during the hemorrhagic shock phase but returns to a similar rate as SHAM models at the completion of the experiment.

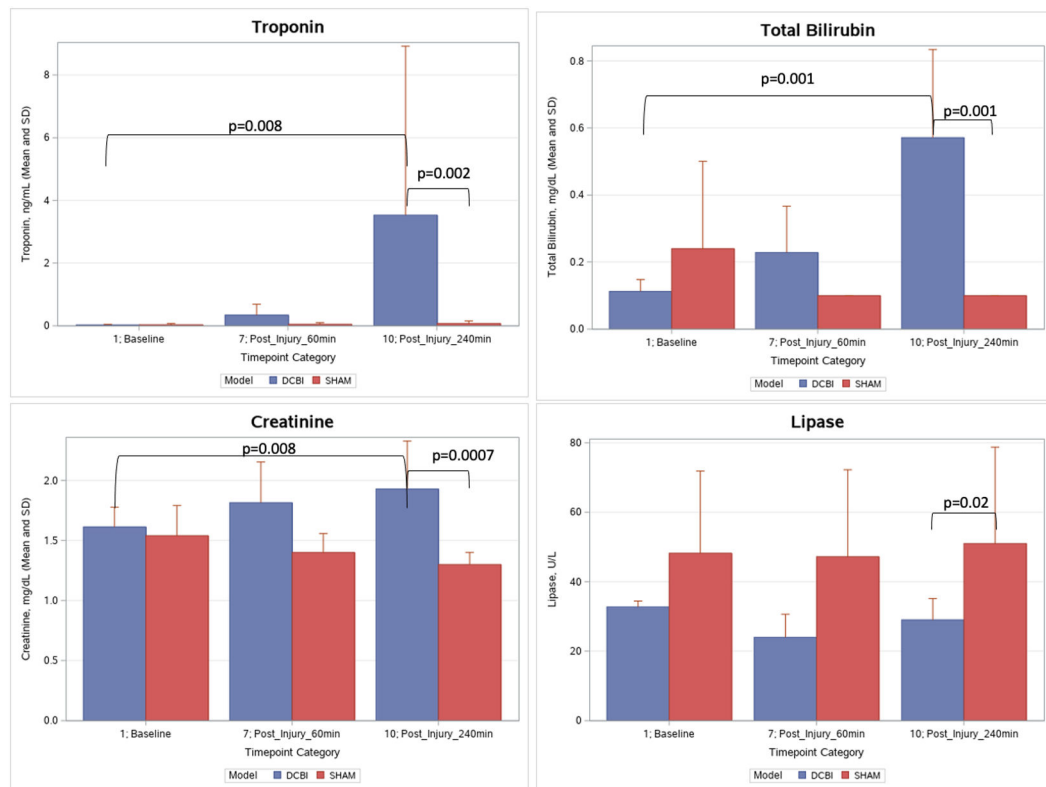


Figure 3. Measure of organ function throughout model.

Troponin, total bilirubin, lipase, and creatinine were measured at baseline, 60min after injury, and at model completion after 240min of observation. There were no significant changes in these labs in the SHAM group. Troponin increased significantly in the DCBI group and was significantly higher than the SHAM group at 240min. Total bilirubin increased significantly in the DCBI group and was significantly higher than the SHAM group at 240min. DCBI final creatinine level was significantly higher than baseline and the corresponding final SHAM level. Lipase trended slightly lower at 240min compared to baseline in the DCBI group, but the final lipase level was significantly lower than the SHAM group.

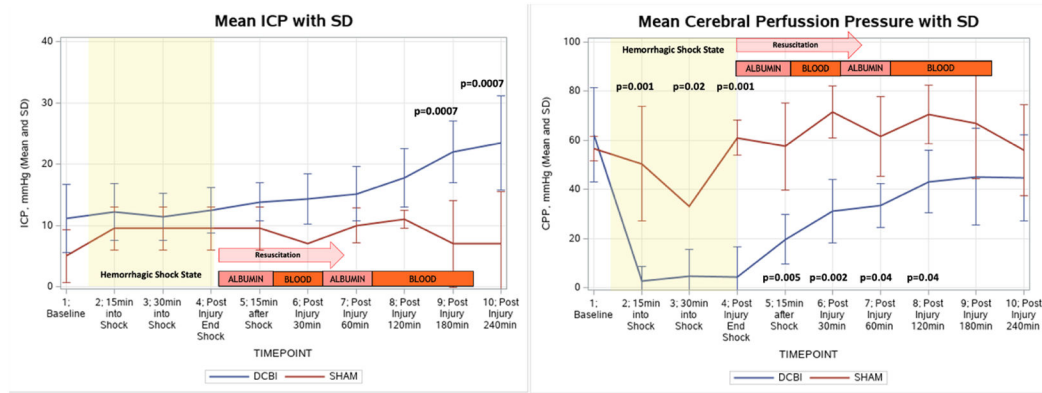


Figure 4. Changes in intracranial pressure and cerebral perfusion pressure. ICP increased significantly in the DCBI model but did not change in the SHAM model. Calculated CPP was significantly lower than baseline at all timepoints once hemorrhagic shock occurred.

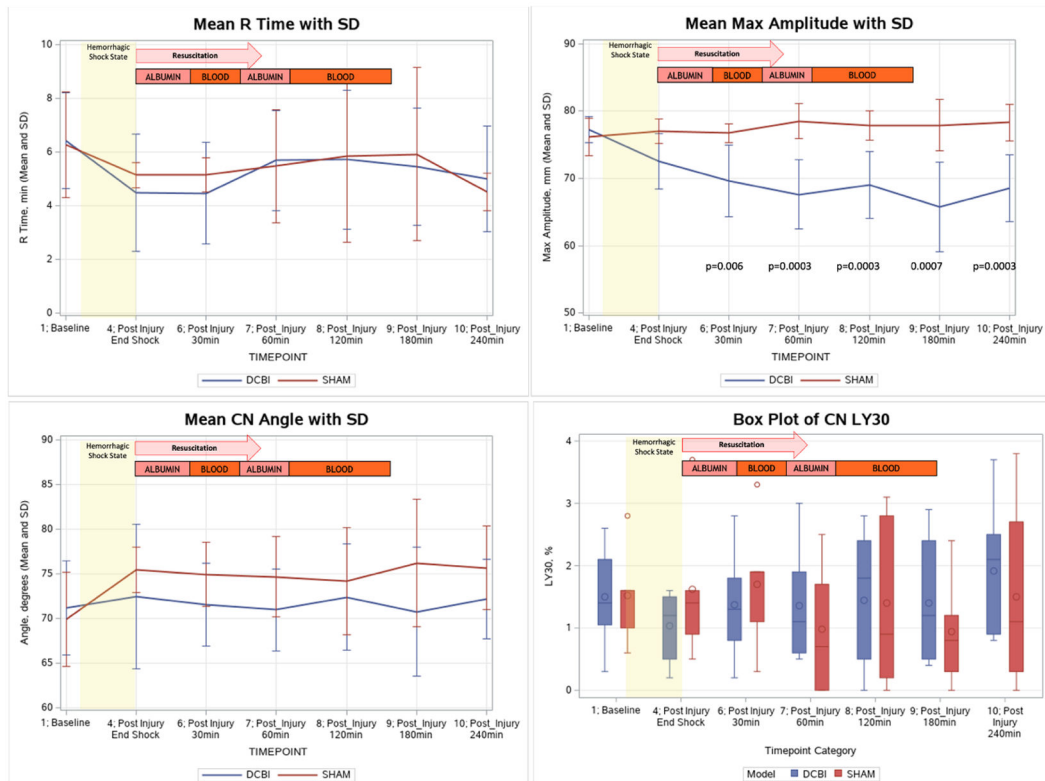


Figure 5. Changes in CN Thromboelastography results.

R time, angle, and LY30 remained at similar levels to baseline for both models. Maximum amplitude decreased significantly in the DCBI model and was significantly lower than the SHAM group at 30min post injury and later.

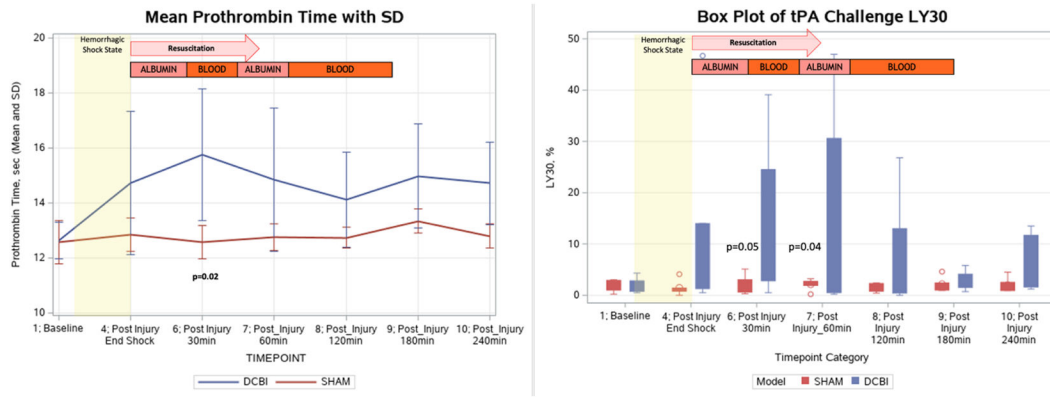


Figure 6. Changes in PT and the tPA Challenge TEG LY30.
 The tPA challenge TEG showed significantly elevated LY30 percentages in the DCBI model compared to the SHAM at 30min and 60min post injury. Significant elevations in PT were detected in the DCBI model compared to the SHAM model at 30min post injury.